

Size-dependent thermal conductivity of zinc oxide nanobelts

Ambarish J. Kulkarni and Min Zhou^{a)}

George W. Woodruff School of Mechanical Engineering, School of Materials Science and Engineering, Georgia Institute of Technology, Atlanta, Georgia 30332-0405

(Received 23 January 2006; accepted 24 February 2006; published online 6 April 2006)

The thermal conductivity of [01 $\bar{1}$ 0]-oriented ZnO nanobelts 19–41 Å in size is characterized over the temperature range of 500–1500 K using the Green-Kubo approach. Values obtained are one order of magnitude lower than that for bulk ZnO single crystal. Surface scattering of phonons and the high surface-to-volume ratios of the nanobelts are primarily responsible for the significantly lower values and the size dependence observed. The conductivity is also found to decrease with temperature and this decrease is attributed to thermal softening of the material, three- and four-phonon processes, and optical phonon interactions. © 2006 American Institute of Physics. [DOI: 10.1063/1.2193794]

ZnO nanowires, nanobelts, and nanosprings are a class of nanostructures with potential applications as ultrasensitive chemical and biological sensors, nanoresonators, nanocantilevers, nanoprobles, and field effect transistors in nanoelectromechanical systems (NEMs).^{1–3} These quasi-one-dimensional (quasi-1D) structures show unique properties sometimes unattainable in bulk. Also, properties often regarded as constants at higher scales display dimensional dependence owing to the high surface-to-volume ratios at the nanoscale. The size dependence of Young's modulus and thermal conductivity is an example.^{4,5} At the nanoscale, electric field density and heat flux are very high; consequently, thermal efficiency and reliability are of great concern. One challenge is that the thermal conductivity is up to two orders of magnitude lower at the nanoscale than what it is in bulk.^{5–8} Characterization of such property variations with size is therefore important.

Most thermal analyses at the nanoscale concern single-element systems whose heat transfer characteristics are primarily dominated by acoustic phonon interactions.^{5–10} However, in compounds such as ZnO higher frequency acoustic and optical phonon interactions play significant roles, especially at higher temperatures. So far, the effects of such phonon interactions have not been systematically characterized and little quantification is available, especially at the nanoscale. In this letter, the thermal conductivity of [01 $\bar{1}$ 0]-oriented ZnO nanobelts (wurtzite structure, $a=3.249$ Å, $c=5.201$ Å)⁴ with lateral dimensions of 19–41 Å over the temperature range of 500–1500 K (melting temperature of ZnO: 2250 K) is quantified. Our approach uses molecular dynamics (MD) and the phonon radiative transport theory^{11,12} for quantifying the contributions of different scattering mechanisms.

The calculations use the Buckingham potential and the Wolf technique for summing Coulomb force contributions.^{13,14} The Green-Kubo approach based on the fluctuation-dissipation theorem is used. Specifically, the thermal conductivity is written as

$$\lambda_{\mu\nu} = \frac{1}{Vk_B T^2} \int_0^\infty \langle J_\mu(t) J_\nu(0) \rangle dt, \quad (1)$$

where V is system volume, T is temperature, k_B is Boltzmann constant, $J_\mu(t)$ is the μ th ($\mu, \nu=1, 2, 3$) component of the heat current, and $\langle J_\mu(t) J_\nu(0) \rangle$ is the autocorrelation function for $J_\mu(t)$ with $\langle \rangle$ denoting ensemble time average. The analysis is limited to temperatures above the Debye temperature θ_D (=420 K for ZnO). Consequently, temperature can be calculated from

$$\frac{3}{2} N k_B T = \frac{1}{2} \sum_{i=1}^N m_i v_i^2, \quad (2)$$

with N being the number of atoms in the system and m_i and v_i being, respectively, the mass and velocity of atom i . Temperatures below θ_D , for which quantum mechanical corrections may be needed, are not considered here.

The simulation cell is 150 Å in length and 21.22 × 18.95, 31.02 × 29.42, or 40.81 × 39.89 Å in the lateral directions. Periodic boundary conditions (PBCs) are specified in the axial direction to approximate the behavior of long belts. Calculations show cell lengths above 100 Å are sufficient for avoiding image effects of PBCs due to truncation of the phonon wavelength spectrum.¹⁵

Figure 1 shows thermal conductivity as a function of temperature for the belts analyzed. The values (3–10 W/m K) are an order of magnitude lower than that for bulk ZnO (~100 W/m K).¹⁶ This significant difference is primarily associated with the high surface-to-volume ratios of the nanobelts. Specifically, the relatively large fractions of surface atoms enhance surface scattering of phonons and decrease the phonon mean free path, resulting in lower conductivity which is proportional to the mean free path. In contrast, the characteristic length for bulk materials is much larger and the effect of boundary scattering is negligible, resulting in larger mean free paths and much higher conductivity values. Also, over 500–1500 K, the conductivity of the 21.22 × 18.95 Å belt is approximately 8%–0.5% lower than that of the 31.02 × 29.42 Å belt and the conductivity of the 31.02 × 29.42 Å belt is approximately 6%–5% lower than that of the 40.81 × 39.89 Å belt.

^{a)} Author to whom correspondence should be addressed; electronic mail: min.zhou@gatech.edu

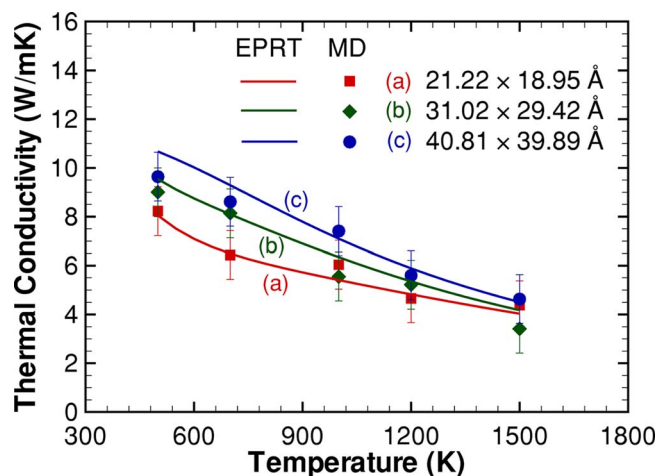


FIG. 1. (Color online) Thermal conductivity as a function of lateral size and temperature.

Surface attributes also affect heat transfer. For the nanobelts, the interlayer spacings between the two outermost layers of (0001) and (2110) planes decrease by 73% and 9%, respectively, relative to the values for bulk ZnO, resulting in higher atomic densities in the surfaces.⁴ Such a deviation from perfect core atomic arrangement alters the surface scattering of phonons and lowers the conductivity. Boundary scattering is also influenced by surface specularity (probability of specular phonon reflection). Berman *et al.*¹⁷ showed that specularity decreases with temperature, causing decreases in conductivity.

Figure 1 shows thermal conductivity decreases with temperature. Between 500 and 1500 K, decreases of about 52% are observed. This effect is attributed to thermal softening and higher frequency phonon interactions at higher temperatures. At each size, the lower lattice stiffness at higher temperatures (due to the nonlinearity of interatomic interactions) results in lower average phonon group velocities and lower levels of heat flux (Fig. 2). Also at higher temperatures, higher frequency acoustic and optical phonon interactions become appreciable, lowering the mean free path and conductivity.

The size and temperature effects can be quantitatively delineated using the equation for phonon radiative transport (EPRT) that accounts for surface phonon interactions.^{11,12} The EPRT for thermal conductivity is¹¹

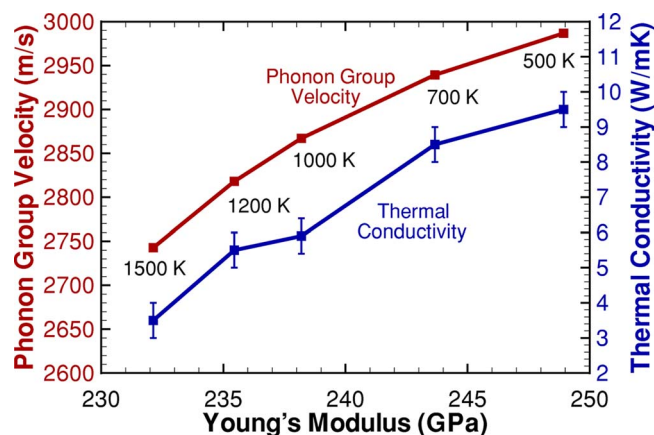


FIG. 2. (Color online) Average phonon group velocity and thermal conductivity of the $31.02 \times 29.42 \text{ \AA}$ belt as functionals of its Young's modulus.

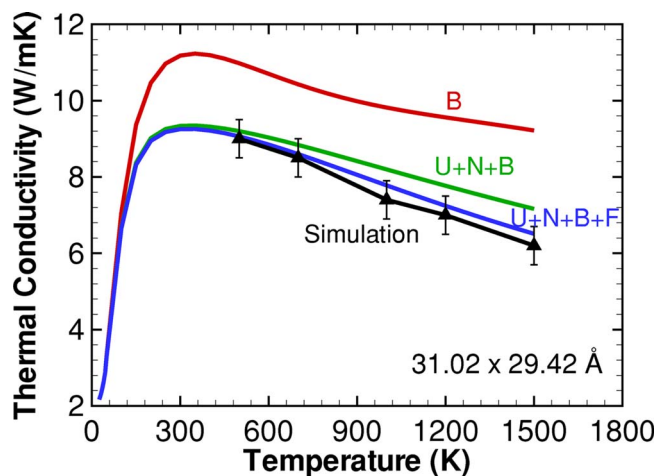


FIG. 3. (Color online) Effects of different scattering mechanisms on the thermal conductivity of the $31.02 \times 29.42 \text{ \AA}$ nanobelt as predicted by EPRT.

$$\kappa(T, d) = \frac{k_B}{2\pi^2 v} \left(\frac{k_B T}{\hbar} \right)^3 \int_0^{\theta_D/T} \frac{x^4 e^x}{(e^x - 1)^2} \tau(T, x) G(\eta) dx, \quad (3)$$

where $x = \hbar\omega/k_B T$, ω is phonon frequency, v is phonon group velocity, \hbar is Planck's constant, $\eta = d/\Lambda(x)$, d is the lateral dimension of the nanobelt, Λ is phonon mean free path, and τ is relaxation time. $G(\eta)$ accounts for the effect of surfaces which gives rise to the size dependence discussed here. This term tends to unity as the lateral size approaches infinity and Eq. (3) reduces to that for bulk materials. The relaxation time τ is calculated using Matthiessen's rule, accounting for boundary, three-phonon (normal and umklapp), and four-phonon scatterings.^{16,18} The specularity and four-phonon relaxation time are determined by fitting Eq. (3) to the results in Fig. 1. Constants related to three-phonon relaxation time are determined from experimental data for bulk ZnO.¹⁶

Figure 3 shows the results for the $31.02 \times 29.42 \text{ \AA}$ belt for cases that account for boundary scattering (B), boundary and three-phonon (normal and umklapp) scattering (B+N+U), and boundary, and three- and four-phonon scattering (B+N+U+F) processes. Over 500–1500 K, boundary scattering is the most dominant process responsible for an ~ 80 –47% decrease in conductivity from the bulk value. A further decrease of $\sim 3\%$ –11% is attributed to three-phonon interactions and another decrease of $\sim 3\%$ –15% is due to four-phonon interactions. At lower temperatures boundary scattering dominates, while above 600 K the three-phonon and four-phonon terms have to be included. The primary reason is that at higher temperatures, the vibration amplitude of atoms becomes sufficiently large so that the effect of three- and four-phonon processes emerges as a significant factor.

Finally, the significant size dependence of thermal conductivity analyzed here echoes a similar trend in mechanical response.⁴ This size dependency of properties at the nanoscale offers potentials for novel applications in NEMSs that rely on thermomechanical responses. Quantification of this phenomenon should provide data and criteria for the design and fabrication of a range of building blocks for nanoscale devices.

Support through NSF CAREER Grant No. CMS9984298 and NSFC Grant No. 10528205 is gratefully acknowledged. Computations are carried out at the

NAVO and ASC MSRCs through AFOSR MURI No. D49620-02-1-0382.

- ¹X. D. Bai, P. X. Gao, Z. L. Wang, and W. G. Wang, *Appl. Phys. Lett.* **82**, 4806 (2003).
- ²E. Comini, G. Faglia, G. Sberveglieri, Z. W. Pan, and Z. L. Wang, *Appl. Phys. Lett.* **81**, 1869 (2002).
- ³W. L. Hughes and Z. L. Wang, *Appl. Phys. Lett.* **82**, 2886 (2003).
- ⁴A. J. Kulkarni and M. Zhou, *Nanotechnology* **16**, 2749 (2005).
- ⁵L. Shi, Q. Hao, C. Yu, N. Mingo, X. Kong, and Z. L. Wang, *Appl. Phys. Lett.* **84**, 2638 (2004).
- ⁶P. Kim, L. Shi, A. Majumdar, and P. L. McEuen, *Phys. Rev. Lett.* **87**, 215502 (2001).
- ⁷D. Li, Y. Wu, P. Kim, L. Shi, P. Yang, and A. Majumdar, *Appl. Phys. Lett.* **86**, 2934 (2003).
- ⁸S. G. Volz and G. Chen, *Appl. Phys. Lett.* **75**, 2056 (1999).
- ⁹P. Jund and R. Jullien, *Phys. Rev. B* **59**, 13707 (1999).
- ¹⁰P. K. Schelling, S. R. Phillpot, and P. Kielinski, *Phys. Rev. B* **65**, 144306 (2002).
- ¹¹X. Lu, W. Z. Shen, and J. H. Chu, *J. Appl. Phys.* **91**, 1542 (2002).
- ¹²A. Majumdar, *J. Heat Transfer* **115**, 7 (1993).
- ¹³D. J. Binks and R. W. Grimes, *J. Am. Ceram. Soc.* **76**, 2370 (1993).
- ¹⁴D. Wolf, P. Keblinski, S. R. Phillpot, and J. Eggebrecht, *J. Chem. Phys.* **110**, 8254 (1999).
- ¹⁵R. C. Picu, T. Borca-Tasiuc, and M. C. Pavel, *J. Appl. Phys.* **93**, 3535 (2003).
- ¹⁶M. W. Wolf and J. J. Martin, *Phys. Status Solidi A* **17**, 215 (1973).
- ¹⁷R. Berman, E. L. Foster, and J. M. Ziman, *Proc. R. Soc. London, Ser. A* **231**, 130 (1955).
- ¹⁸Y. P. Joshi, M. D. Tiwari, and G. S. Verma, *Phys. Rev. B* **1**, 642 (1970).